Magnetic relaxation and thermal properties of a two-dimensional array of dipolar-coupled nanoparticles

2007 J. Phys.: Condens. Matter 19 276203

(http://iopscience.iop.org/0953-8984/19/27/276203)

IOP PUBLISHING JOURNAL OF PHYSICS: CONDENSED MATTER

J. Phys.: Condens. Matter **19** (2007) 276203 (19pp) doi:10.1088/0953-8984/19/27/276203

Magnetic relaxation and thermal properties of a two-dimensional array of dipolar-coupled nanoparticles

W Figueiredo[1,2] **and W Schwarzacher**[2]

[1] Departamento de Física, Universidade Federal de Santa Catarina, 88040-900, Florianópolis, SC, Brazil
[2] H H Wills Physics Laboratory, Tyndall Avenue, Bristol BS8 1TL, UK

Received 27 April 2007, in final form 30 May 2007
Published 20 June 2007
Online at stacks.iop.org/JPhysCM/19/276203

Abstract

We investigate through Monte Carlo simulations the thermal properties of a triangular array of identical magnetic nanoparticles with random uniaxial anisotropy axes in three dimensions. They are coupled by dipolar forces and we determine the blocking temperature of the system as a function of the anisotropy strength and magnitude of the dipolar coupling. We calculate the magnetization, susceptibility, specific heat and Binder cumulant as a function of temperature, and we see that, in the non-interacting case, these properties exhibit a maximum at the blocking temperature. We have found that the increase of blocking temperature is related to an increase in the effective energy barrier due to the dipolar interactions. We have also determined the dependence of the remanence and coercive field as a function of temperature and dipolar strength. At very low temperatures, the coercive field displays a minimum as a function of dipolar strength. The magnetic relaxation is studied as a function of temperature and dipolar strength for an assembly of nanoparticles possessing the same uniaxial anisotropy energy. We have also considered the behaviour of the almost non-thermal relaxation that occurs at the very beginning of the relaxation process as a function of the dipolar coupling strength.

1. Introduction

The pioneering studies of Stoner and Wohlfarth [1], Néel [2] and Brown [3], on the magnetization reversal of single-domain particles with very large magnetic moments through thermal fluctuations across energy barriers, appeared until recently to be of purely academic interest. However, the development of new techniques to produce nanostructured single-domain magnetic particles [4–6] permitted the correctness of these ideas to be verified. Indeed, samples of high quality have been produced for which the individual nanoparticles are

coated by non-magnetic layers to prevent the exchange coupling between nearest neighbour particles [5, 7–11]. Each individual nanoparticle is formed by hundreds or thousands of atomic magnetic moments strongly coupled by exchange interactions. The direction of the resulting magnetic dipole is determined by the uniaxial anisotropy, which includes shape and magnetocrystalline contributions. If the degree of dilution of the sample is high, the nanoparticles behave as giant magnetic dipoles and their dynamics are dictated only by the external applied magnetic fields, uniaxial anisotropy and coupling with the heat bath. This is the proper scenario to test the fundamental ideas of the founders of the superparamagnetic theory.

When the dilution is not so low, long-range magnetic dipolar forces among the nanoparticles must be taken into account to correctly describe the thermodynamical behaviour of these systems. Due to the dipolar interactions, the otherwise purely uniaxial anisotropy energy barrier seen by each nanoparticle is modified. It is still a matter of debate in the literature the way this change occurs. Even in the limit of weak dipolar interactions, in some experiments [12] the blocking temperature increases with concentration while in others it decreases [13].

From a theoretical point of view the array topology of the nanoparticles is very important. Luttinger and Tisza [14] have shown that the lowest energy state of a collection of classical dipoles is ferromagnetic in a face centred cubic lattice, whereas it is antiferromagnetic in a simple cubic lattice. In two dimensions it is well established that a square lattice of classical point dipoles exhibits an antiferromagnetic arrangement of the moments [15, 16], while for a triangular lattice the arrangement is ferromagnetic [17, 18].

Depending on which property we are analysing, the role played by the dipolar interactions in the effective energy barrier of the nanoparticle appears different. For instance, in the case of zero-field-cooled (ZFC) curves, the blocking temperature increases with the strength of the dipolar interactions, suggesting that the effective energy barrier seen by the nanoparticle also increases [19]. On the other hand, in the case of the magnetic relaxation process from a saturated state, the dipolar interactions effectively reduce the barrier height seen by the nanoparticles [20].

In this paper we investigate the thermodynamic properties of a set of identical nanoparticles in a two-dimensional triangular lattice through Monte Carlo simulations. The easy axes are randomly oriented in three dimensions and the particles interact through a long-range magnetic dipolar interaction. From the ZFC curves we calculate, as a function of temperature and uniaxial anisotropy, the magnetization, susceptibility, specific heat and Binder cumulant. For the non-interacting case, we see that these properties exhibit a maximum at the same temperature. The remanence and the coercive field were also determined as a function of temperature and strength of the dipolar interactions. The decay of the magnetization from a saturated state, at different temperatures, permitted us to calculate the relaxation times for the interacting and non-interacting systems. For a limited range of temperatures, we have seen that in this particular relaxation process the effective energy barrier of the interacting system is lower than that of the non-interacting one. An important aim of the present work is to relate the effects of dipolar interactions on the thermodynamic properties recorded in ZFC experiments, for which the initial state is completely random, to those found in the relaxation of the magnetization from well ordered initial states.

The text is organized as follows: in section 2 we present the model and details concerning the Monte Carlo simulations; in section 3 we present the results for the thermodynamic properties from the ZFC curves; in section 4 we describe the results for the relaxation of the magnetization considering the ultrafast and slow processes; finally, in section 5, we summarize our conclusions.

2. Model and Monte Carlo simulations

We consider a two-dimensional triangular array of identical nanoparticles in the xy plane. Each one possesses a uniaxial anisotropy with its easy axis pointing randomly in the three-dimensional space. The magnitude of the anisotropy is given by $d = KV$, where K is the anisotropy energy per unit volume and V is the volume of the particle, which we assume to be the same for all the particles. The magnetic moment of the ith particle is written as $\vec{\mu}_i = \mu\vec{S}_i$, where $\vec{S}_i$ is a unit vector, $|\vec{S}_i| = 1$, and $\vec{S}_i = (S_{ix}, S_{iy}, S_{iz})$. We also write μ in the form $\mu = M_s V$, where M_s is the particle magnetization. An in-plane external magnetic field of magnitude H is applied along the x-direction of the triangular lattice, which we choose to be parallel to a side of the conventional unit cell. The particles interact via a two-pair dipolar term, and the magnitude of the dipolar energy is written as a function of the parameter $g = \mu^2/a^3$, where a is the lattice parameter. The corresponding Hamiltonian for a set of N particles is

$$\mathcal{H} = \frac{1}{2}g\sum_{i=1}^{N}\sum_{j\neq i}^{N}\left[\frac{\vec{S}_i\cdot\vec{S}_j}{r_{ij}^3} - 3\frac{(\vec{S}_i\cdot\vec{r_{ij}})(\vec{S}_j\cdot\vec{r_{ij}})}{r_{ij}^5}\right] - \sum_{i=1}^{N} hS_{ix} - \sum_{i=1}^{N} d(\vec{e}_i\cdot\vec{S}_i)^2, \tag{1}$$

where r_{ij} is the distance separating the magnetic moments at the sites i and j, which is measured in units of the lattice parameter a and we have also defined that $h = \mu H$. The vector $\vec{e}_i$ is the unitary vector in the direction of the easy axis for the particle at the site i. An important parameter to describe the effect of dipolar interactions on the magnetic properties of the system is the ratio $\alpha = g/d$. In this work we compare our results with those found for a system of magnetoferritin nanoparticles, which present a very narrow size distribution and the easy axes are randomly distributed over the sample. It is an interesting nanoparticle to probe the effect of the dipolar interactions, because its 2 nm protein shell prevents contact between the magnetic cores of nearest neighbour nanoparticles. Arrays of magnetoferritin particles were prepared on coated Cu TEM grids and studied by TEM and SQUID magnetometry [9, 21]. In the dispersed sample, the calculated mean interparticle separation was 130 nm, while in the aggregated sample, the magnetoferritin particles were in contact. The magnetoferritin particles are spherical with an average diameter of 12 nm, while the diameter of magnetic core is $D = 8$ nm. The estimated anisotropy energy density is $K = 4.2 \times 10^5$ erg cm^{-3}, while the magnetization is $M_s = 500$ emu cm^{-3}. Therefore, $\alpha = \frac{\pi}{6}\frac{M_s^2}{K}(\frac{D}{a})^3$, and for the concentrated case, where particles touch each other, $a = 12$ nm, the estimated value of α is 0.1. For the magnetoferritin system the blocking temperature of the well dispersed and most aggregated samples is 21.5 K and 28 K, respectively.

Studies on the magnetic properties of nanoparticles have been performed at zero temperature, exploring the hysteresis phenomenon and structure of the monolayer [17, 22–24], and at finite temperatures, where besides hysteresis other properties have also been investigated. Most of the calculations at finite temperature were performed by employing Monte Carlo simulations. For instance, effects of packing geometries [25], tunnelling magnetoresistance [26], reversible transverse susceptibility [27], magnetic relaxation [20, 28–31] and finite size effects [32, 33], are some of the problems that have received some attention in recent years. Analytical expressions for the total magnetic moment and correlation functions as a function of temperature and field have also been calculated for molecular magnets containing a very small number of interacting moments [34, 35].

We have carried out Monte Carlo simulations to study the thermal properties from the ZFC initial state as well as the magnetic relaxation. We have taken a system of linear size $L = 21$ on a triangular lattice, with 441 magnetic moments, and we assumed free boundary conditions in our calculations. The question of the boundary conditions was analysed in detail in the work of Kechrakos and Trohidou [25] in their study of the remanence as a function of

the dipolar interaction strength at very low temperatures. In order to determine the equilibrium properties of the system starting from the ZFC initial state, we minimize its free energy by using the Monte Carlo technique and the well known Metropolis algorithm [36]. According to this algorithm a given magnetic moment is selected at random, and we try to move it to a new position in such a way that the deviation from the old state is random but within a maximum solid angle. We calculate the change in energy of the system (ΔE), and if $\Delta E \leqslant 0$ the transition to the new configuration is accepted. On the other hand, if $\Delta E > 0$ the transition to the new configuration is made with probability $\exp(-\Delta E/k_{\mathrm{B}}T)$. This is the most expensive part of the simulation, because after the transition we need to recalculate the dipolar field acting on all the other particles of the system. In each Monte Carlo step (MCS), we performed $N = 441$ (N is the number of magnetic moments of the system) trials to flip the magnetic moments. To calculate the average magnetic properties we considered 10^4 MCSs, where the first 2×10^3 MCSs were discarded due to the thermalization process. This number of MCSs to reach the equilibrium state was achieved by taking a maximum solid angle variation equal to 0.1π, where approximately 50% of the attempted moves were successful. Due to the thermal fluctuations and random direction of the easy axis, we have taken a minimum of 50 and a maximum of 200 samples to determine the thermal properties. On the other hand, each sample is selected for a ZFC experiment only when its initial total magnetization is less than 10^{-3}.

In our algorithm we calculated the average magnetization per particle, as well as its components in the x, y and z directions, as a function of temperature, uniaxial anisotropy and dipolar strength. These average values were obtained firstly by calculating the mean values of the magnetic moments of the system for each MCS after the thermalization process:

$$M_x = \frac{1}{N}\sum_{i=1}^{N} S_{ix}, \tag{2}$$

$$M_y = \frac{1}{N}\sum_{i=1}^{N} S_{iy}, \tag{3}$$

$$M_z = \frac{1}{N}\sum_{i=1}^{N} S_{iz}, \tag{4}$$

$$M_{\mathrm{tot}} = \sqrt{M_x^2 + M_y^2 + M_z^2}. \tag{5}$$

Afterwards, these averages are taken by considering all the Monte Carlo steps, after thermalization. Finally, an average is performed over all the selected samples. We have also calculated the following physical quantities: the susceptibility from the fluctuation of the magnetization,

$$\chi = \frac{N}{T}(\langle {M_x}^2\rangle - \langle |M_x|\rangle^2), \tag{6}$$

the specific heat from the fluctuation of the total energy (per magnetic moment) E,

$$C = \frac{N}{T^2}(\langle E^2\rangle - \langle E\rangle^2), \tag{7}$$

and the Binder cumulant [37]

$$B = 1 - \frac{\langle {M_x}^4\rangle}{3\langle {M_x}^2\rangle^2}. \tag{8}$$

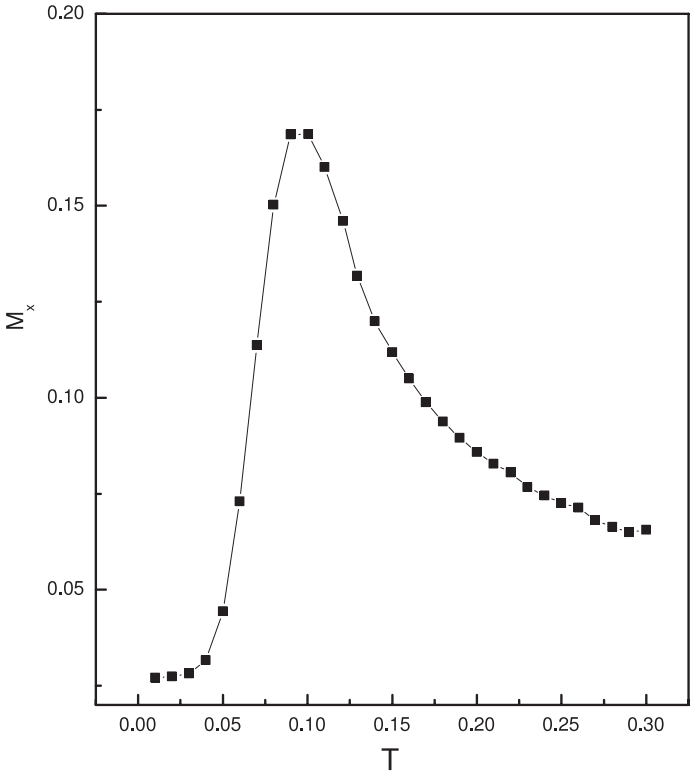

Figure 1. Zero-field-cooled magnetization versus temperature for a non-interacting system ($\alpha = 0$) and anisotropy energy $d = 0.6$. The external magnetic field is $h = 0.05d$. The line serves as a guide to the eye.

3. Thermodynamic properties

We initially consider a zero-field-cooled sample and we apply a very small magnetic field in the x-direction. In our simulations we have taken for this field the value $h = 0.05d$, where d is the barrier height due to the uniaxial anisotropy. For each value of d the magnetization is almost zero at very low temperatures. Then, increasing the temperature, some magnetic moments become unblocked, and a net magnetization appears in the field direction. Further increasing the temperature, the magnetization reaches a maximum value, which is defined as the blocking temperature of the system. For temperatures higher than the blocking one, the magnetization decreases for increasing values of temperature and the system is in the superparamagnetic state.

Figure 1 shows the behaviour of the magnetization as a function of temperature for the particular case $d = 0.6$ and non-interacting particles, $\alpha = 0$. We find a well defined peak in the magnetization curve at $T = 0.085$, which corresponds to the blocking temperature for this particular value of the uniaxial anisotropy. We are taking Boltzmann's constant equal to one in our energy units. Figures 2–4 are the corresponding plots of the susceptibility, specific heat and Binder cumulant as a function of temperature, respectively. The maximum observed in the susceptibility and specific heat curves occurs almost at the same temperature as for the magnetization. The susceptibility and the specific heat are governed by the second- and fourth-order moments of the magnetization along the field direction, respectively. In the case of non-

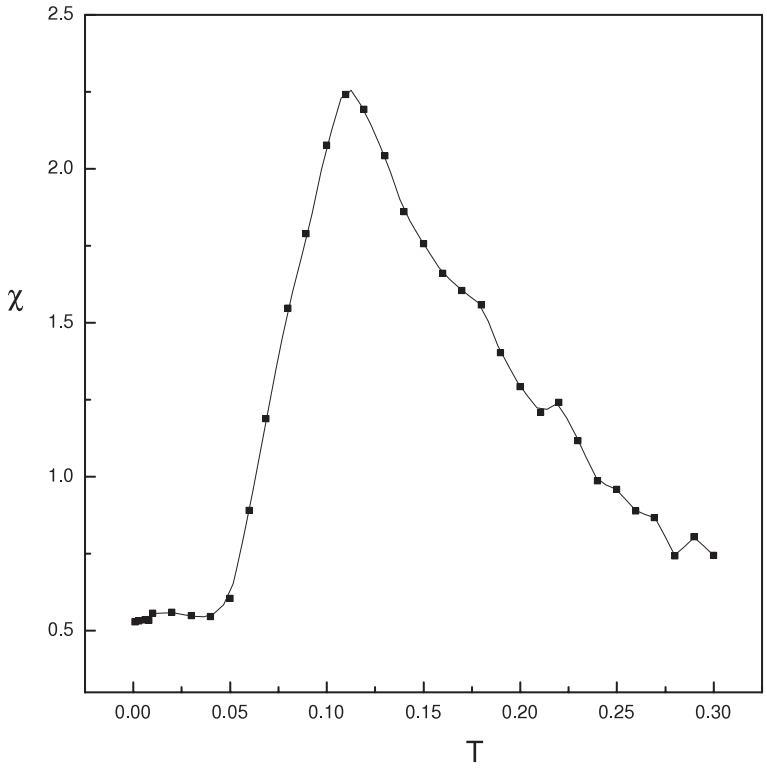

Figure 2. Zero-field-cooled susceptibility versus temperature for a non-interacting system ($\alpha = 0$) and anisotropy energy $d = 0.6$. The external magnetic field is $h = 0.05d$. The line serves as a guide to the eye.

interacting particles the specific heat can be written as

$$C = \frac{d^2}{T^2}(\langle {M_x}^4 \rangle - \langle {M_x}^2 \rangle^2), \tag{9}$$

and this type of fluctuation behaves in the same way as the fluctuation of the susceptibility, although the specific heat curve is more broadened in the region of the maximum than that of the susceptibility. We have not included in our plots the error bars. For temperatures below the blocking temperature the error bars are of the size of the symbols used or smaller. However, for temperatures larger than the blocking one, when the system is in the superparamagnetic state, the thermal fluctuations are very large and the error bars are bigger than the corresponding symbols. These errors can be reduced by increasing the number N of magnetic moments of the system and the number of independent samples, although this procedure will not change the value of the blocking temperature. The interplay between second- and fourth-order moments appears more clearly in the Binder cumulant, figure 4, which also exhibits a broad local maximum near the blocking temperature. As the particles become unblocked due to the thermal fluctuations, the Zeeman energy decreases up to near the blocking temperature, while the energy due to the uniaxial anisotropy increases. It is the competition between these two energy contributions that allows this interesting behaviour. In the context of phase transitions, where the magnetic field is zero, the Binder cumulant is always a decreasing function of temperature.

When the dipolar interactions are taken into account a different scenario appears. Although we can find a well defined maximum in the curve of the magnetization versus temperature

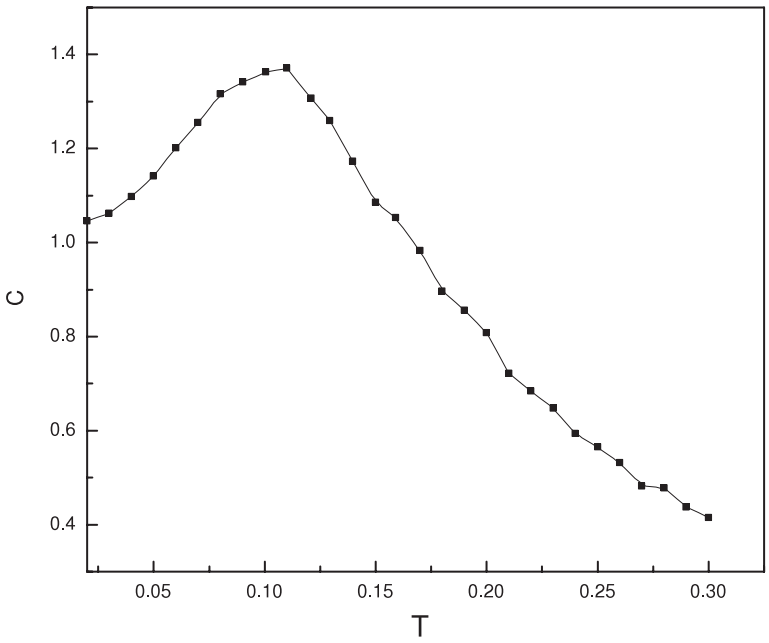

Figure 3. Zero-field-cooled specific heat as a function of temperature for a non-interacting system ($\alpha = 0$) and anisotropy energy $d = 0.6$. The external magnetic field is $h = 0.05d$. The line serves as a guide to the eye.

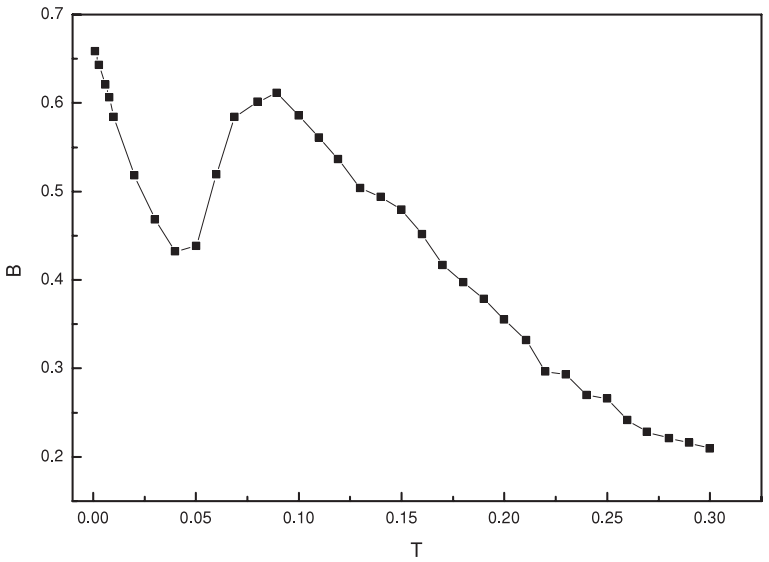

Figure 4. Zero-field-cooled Binder cumulant as a function of temperature for a non-interacting system ($\alpha = 0$) and anisotropy energy $d = 0.6$. The external magnetic field is $h = 0.05d$. The line serves as a guide to the eye.

for each value of d, the fluctuations are large for the other properties. This occurs because in the triangular lattice the dipolar interactions favour a ferromagnetic alignment of the

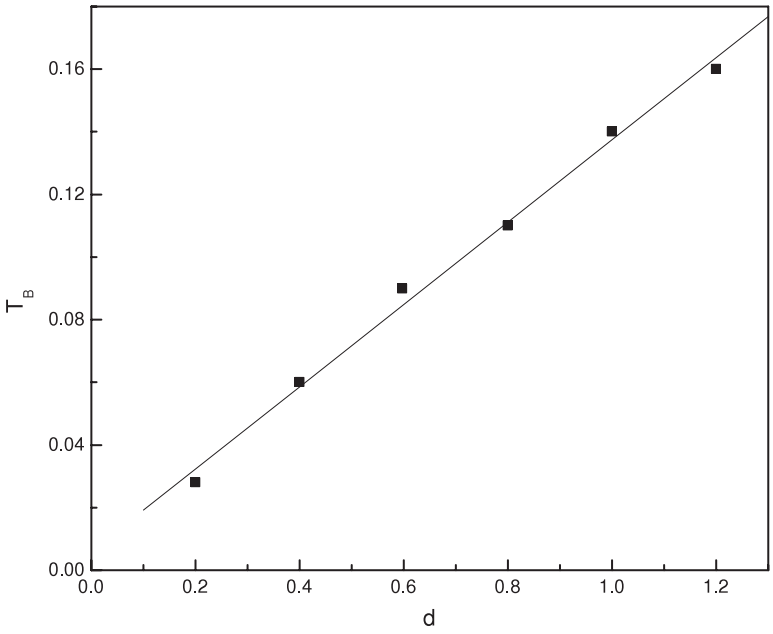

Figure 5. Blocking temperature as a function of the anisotropy energy for a non-interacting system ($\alpha = 0$) along with the best fit to the data points.

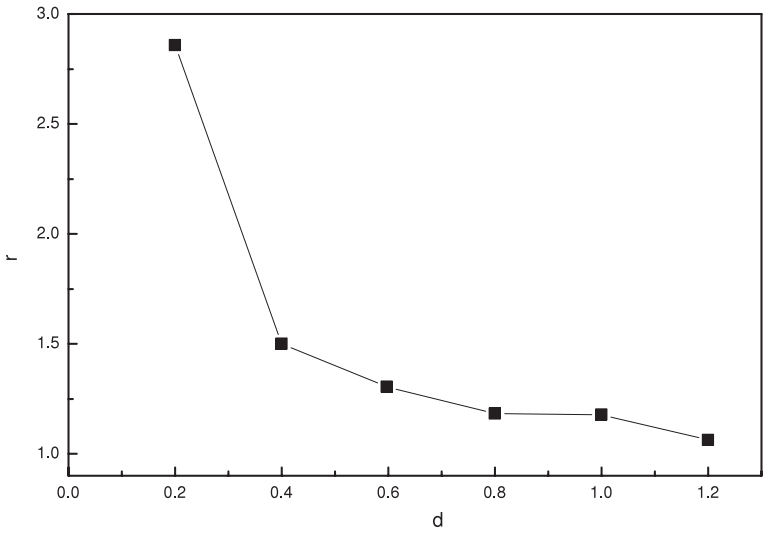

Figure 6. Ratio between the blocking temperatures of the interacting ($\alpha = 0.1$) and non-interacting ($\alpha = 0$) systems as a function of the anisotropy energy. The line serves as a guide to the eye.

magnetic moments and, even at very low temperatures, there is a non-zero component of the magnetization in the direction perpendicular to the small field. Fluctuations of the magnetic moments in the field direction are now correlated with those in the transverse direction.

We plot in figure 5 the blocking temperature versus the barrier height for the non-interacting case. From a linear fit we find the slope $d/T_B = 7.69$. In figure 6 we show the

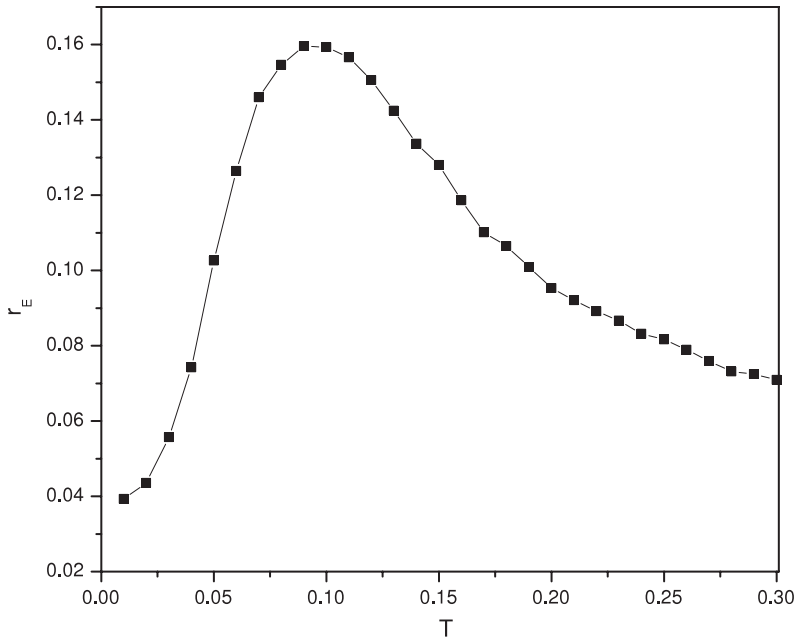

Figure 7. Ratio between the dipolar and uniaxial anisotropy energies as a function of temperature for $\alpha = 0.1$ and $d = 0.6$. The line serves as a guide to the eye.

dependence of r, the ratio between the blocking temperatures for the interacting ($\alpha = 0.1$) and non-interacting ($\alpha = 0$) systems. As commented earlier, the blocking temperature of the interacting system was determined from the maximum in the magnetization versus temperature curve.

When the barrier height becomes large the ratio between the blocking temperatures approaches one. As for each value of d the parameter α is always taken equal to 0.1, we can look at this plot as showing the decrease [38] in the concentration of the number of particles for increasing values of d. Let us compare these results with those known for the magnetoferritin system [21]. The blocking temperature of the well dispersed and most aggregated samples is 21.5 K and 28 K, respectively. The mean distance between two nearest neighbour particles in the well dispersed sample is 120 nm, which gives $\alpha = 10^{-4}$, that is, the well dispersed sample is non-interacting and we assume for it the value $\alpha = 0$. In figure 6, the value $d = 0.6$ accounts for the correct ratio between the blocking temperatures of the most aggregated ($\alpha = 0.1$) and well dispersed ($\alpha = 0$) magnetoferritin samples. This is only an estimate, because in the experimental system the uniaxial anisotropy takes a broad range of values. The effect of the dipolar interactions is to increase the effective energy barrier height seen by the nanoparticles in the ZFC experiments performed on samples with a triangular arrangement of magnetic dipoles. This effect can be seen in figure 7, where we plot the ratio between the dipolar and uniaxial anisotropy energies versus temperature for $\alpha = 0.1$ and $d = 0.6$. Indeed, an increase in this ratio is observed up to temperatures around the blocking temperature of the system.

An important question arises when we try to compare the timescales of the experiments and the Monte Carlo simulations. Although Monte Carlo simulations are useful to take into account thermal fluctuations, the unit of time in the Monte Carlo simulations (MCSs) does not correspond to the real time in the laboratory. The blocking temperature of a system is a property that depends on the timescale of the experiment. For example, in the case of the magnetoferritin

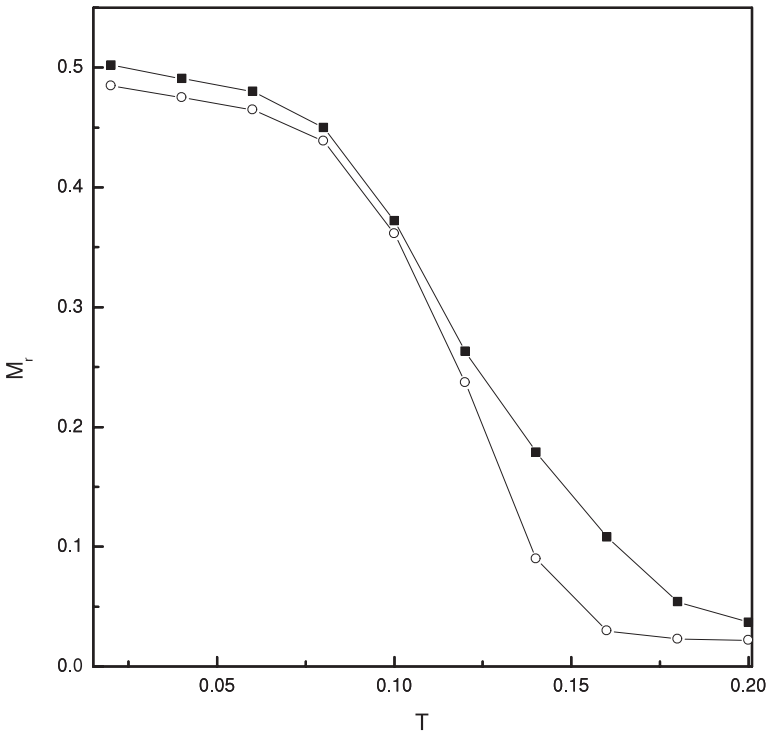

Figure 8. Remanence of the interacting ($\alpha = 0.1$, solid squares) and non-interacting ($\alpha = 0$, open circles) systems as a function of temperature for $d = 1.0$. The lines serve as a guide to the eye.

system, typical measurements employing a SQUID apparatus take a time $t^L \approx 1000$ s, and therefore the ratio of the energy barrier to blocking temperature is estimated to be $d/T_B \approx 30$. We have found in our Monte Carlo simulations that $d/T_B = 7.69$. Then, assuming that the attempt frequency is the same in the experiments and in the simulations [39], we see that the real time t^S corresponding to the length of the simulations is $t^S \approx 200$ ns. This means that performing a simulation with 10^4 MCSs corresponds to a time in the laboratory of only 200 ns. The only effect of increasing the number of MCSs would be an increase in ratio d/T_B and in t^S. However, despite the real time involved in the simulations being so small compared with the laboratory time, the Monte Carlo calculations capture the essence of the experiment concerning the underlying thermal fluctuations.

Next, we consider the remanence and coercivity of the system. We determined the remanence by letting the magnetic moments of the nanoparticles relax, in a zero external field, from an initial state where all the moments are aligned in the x-direction, that is, the initial state is given by ($S_{ix} = 1$, $S_{iy} = 0$, $S_{iz} = 0$). We also considered 10^4 MCSs for the system to reach equilibrium, although at very low temperatures equilibrium is easily achieved within 500 MCSs. We considered 200 samples to allow different realizations of the random axis distribution. We show in figure 8 the remanence as a function of temperature for $\alpha = 0$, the non-interacting case, and also for $\alpha = 0.1$. At zero temperature, the remanence of the system of non-interacting particles is $1/2$, due to the random distribution of uniaxial axes in three dimensions. We also note that at zero temperature the remanence of the system of interacting nanoparticles is larger than for the non-interacting particle system. This is a consequence of the dipolar interactions in a triangular lattice, where the lowest energy state presents a

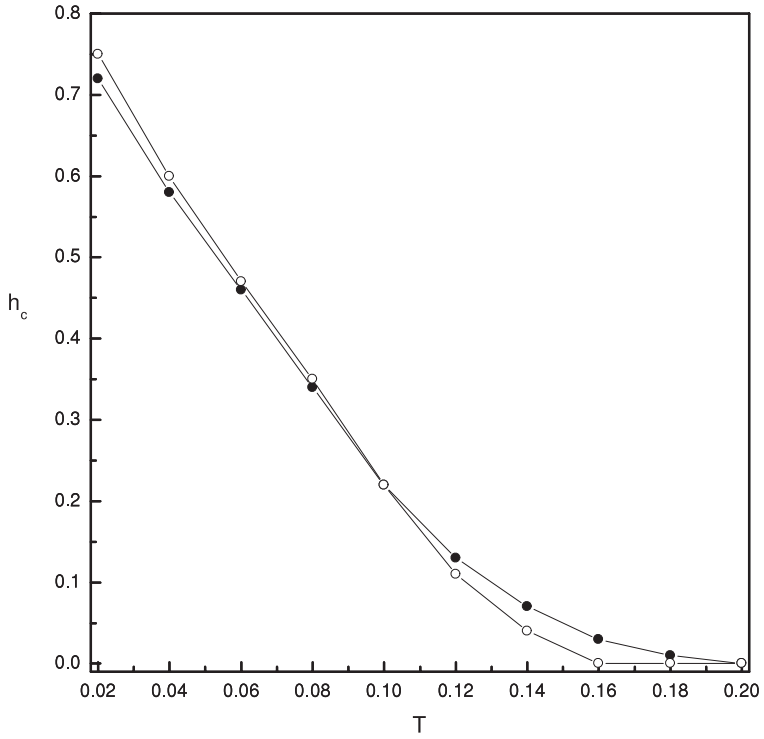

Figure 9. Coercive field of the interacting ($\alpha = 0.1$, solid circles) and non-interacting ($\alpha = 0$, open circles) systems as a function of temperature for $d = 1.0$. The lines serve as a guide to the eye.

ferromagnetic ordering. Compared with the non-interacting case, we see that the decay is smoother and presents an inflection point at temperatures significantly further from T_B. The blocking temperature can also be defined as being the temperature at which the remanence goes to zero. We see that the blocking temperatures for the interacting and non-interacting systems appear slightly larger than those seen in figures 5 and 6, for $d = 1.0$.

The coercivity is defined by the value of the external magnetic field for which the x-component of the magnetization, at the end of the simulation, changes its sign after we start from the uniform distribution of magnetic dipoles ($S_{ix} = 1$, $S_{iy} = 0$, $S_{iz} = 0$) at $t = 0$. The external magnetic field is applied in the x-direction. We also considered 200 different samples and waited 10^4 MCSs to determine the coercive field. In figure 9 we show the behaviour of the coercive field as a function of temperature for $\alpha = 0.0$ and 0.1. At very low temperatures, the coercive field is smaller for interacting particles. It crosses the non-interacting curve at intermediate temperatures and decays smoothly at high temperatures. As in the case of remanence, we can also define the blocking temperature as where the coercive field vanishes. This definition fits better with the results shown in figures 5 and 6 for $d = 1.0$.

We show in figure 10 the plot of the coercive field as a function of the dipolar strength α at very low temperatures ($T = 10^{-4}$). We observe a minimum in this curve near $\alpha = 0.3$ and we find that the decrease of the coercive field is only 13% from its value relative to the non-interacting case. On the other hand, the decrease found by Russier [17] for the same value of α is 75%. We believe that the unusual behaviour we find for the coercive field at very low temperatures is due to the use of free boundary conditions in our simulations. The question of boundary conditions in Monte Carlo simulations has been considered by Kechrakos and

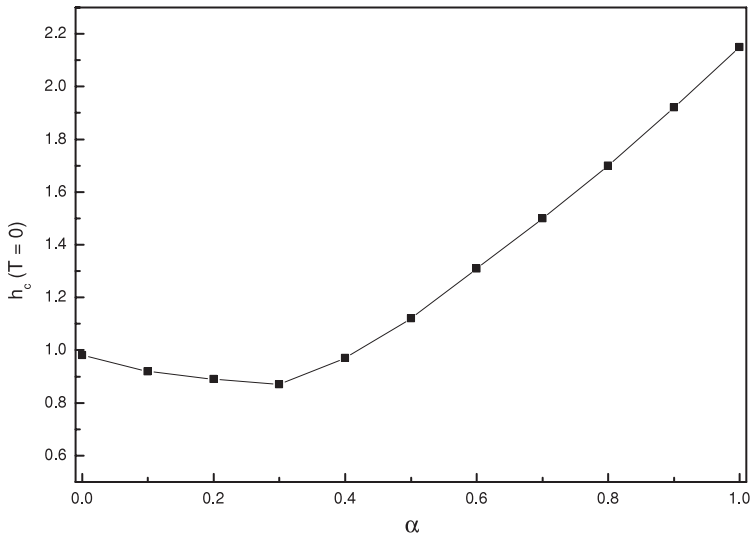

Figure 10. Zero-temperature coercive field as a function of the dipolar strength for $d = 1.0$. The line serves as a guide to the eye.

Trohidou [25, 26]. They have shown [25] that in the case of a simple cubic structure and weak dipolar interactions remanence increases with particle concentration when using periodic boundary conditions, while it decreases when free boundary conditions are used. In the case of a triangular array of particles, they observed [26] that the trends in magnetization and tunnelling magnetoresistance remain unchanged with the use of free or periodic boundary conditions, provided the dipolar field is weak. However, for values of $\alpha > 0.3$ they pointed out that demagnetization effects must be taken into account.

We show in figure 11 the plot of the absolute value of the component of the magnetization transverse to the field as a function of α when $M_x = 0$. While the M_y component is zero for $\alpha = 0$, its value rises to 0.11 when $\alpha = 0.1$. Therefore, for $\alpha \neq 0$, the computed value of the coercive field does not correspond to a zero total magnetization. For completeness, we also show in figure 12, the energy contributions as a function of α calculated at the coercive field at zero temperature. While the dipolar energy is a monotonically decreasing function of α, the uniaxial anisotropy energy exhibits a minimum at the same point as the coercive field does. We tried many random distributions of easy axes in our calculations. Although we could expect a ferromagnetic state extending over the whole system only for large values of the dipolar strength [17], this is opposed by the demagnetizing field from the free poles at the borders of the system, which result from our choice of free boundary conditions. This is true even for moderate values of dipolar coupling, as we can see for the large values of the component M_y at the coercive field.

Another manifestation of the use of free boundary conditions can be seen in figure 13, where we plot the three components of the remanent magnetization as a function of α for $T = 10^{-4}$. The out of plane component M_z is almost zero even for the non-interacting case and decreases even more as α increases. The two in-plane components of the total magnetization present different behaviours. The x-component, M_x, slightly increases from the value $1/2$, which is the well known value for a non-interacting system with completely random uniaxial axes in three dimensions, up to near $\alpha = 0.2$, and then decreases again for $\alpha > 0.3$, to a value near $1/2$. On the other hand, the absolute value of the transverse component of the

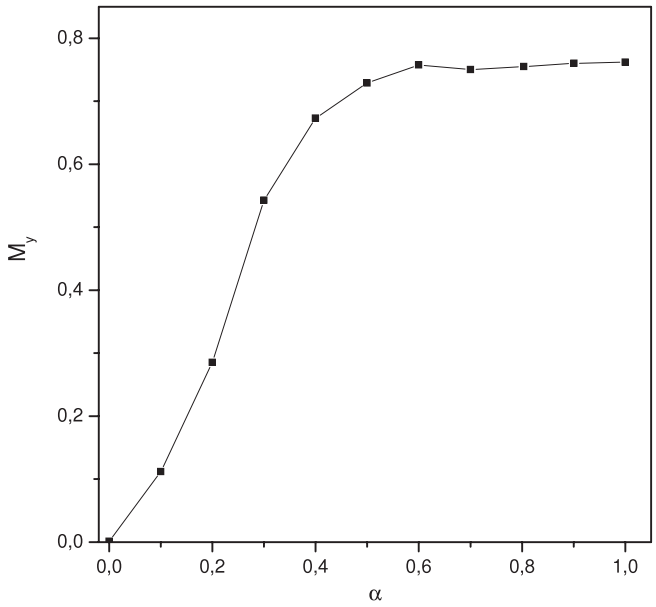

Figure 11. M_y component of the total magnetization transverse to the coercive field as a function of the dipolar strength for $d = 1.0$. The line serves as a guide to the eye.

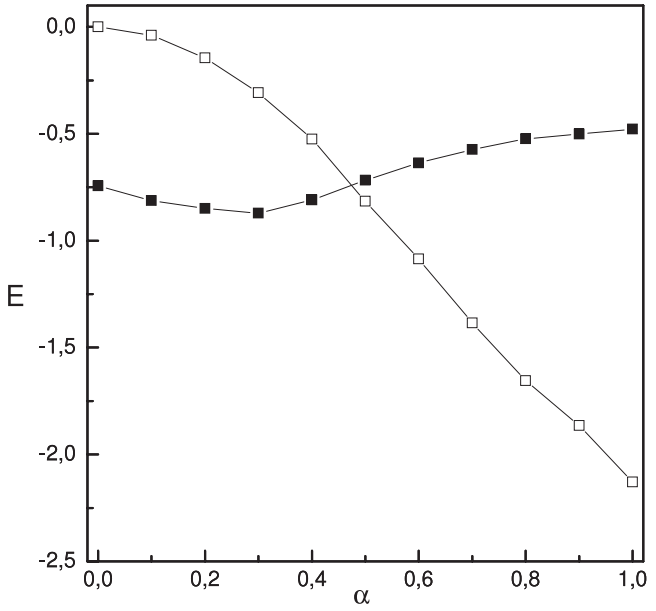

Figure 12. Uniaxial anisotropy (solid squares) and dipolar (open squares) energies per particle, calculated at the coercive field, as a function of the dipolar strength for $d = 1.0$. The lines serve as a guide to the eye.

magnetization, M_y, is an increasing function of α. Again, near $\alpha = 0.3$, we observe a crossing of the curves M_x and M_y, showing the importance of the transverse component of the magnetization when free boundary conditions are used.

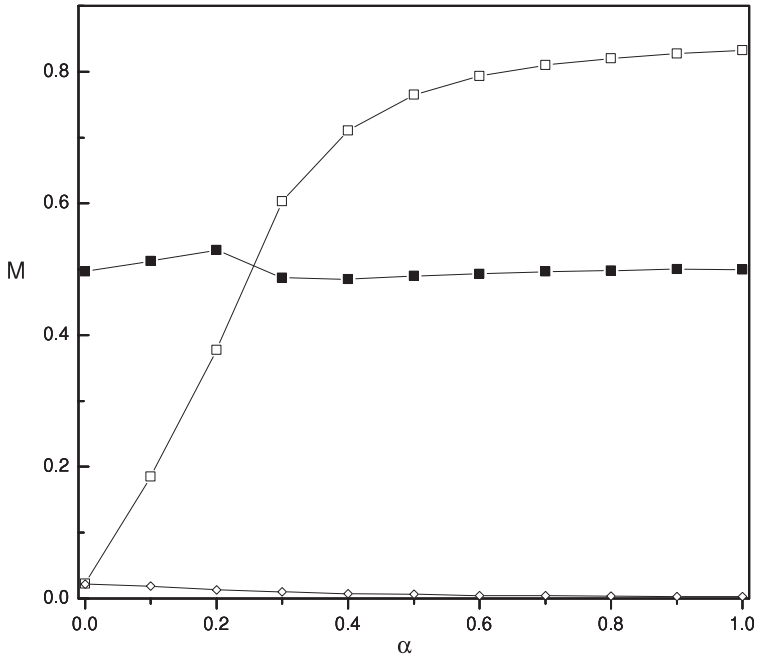

Figure 13. Components of total magnetization as a function of the dipolar strength for $d = 1.0$. M_x (solid squares), M_y (open squares) and M_z (open diamonds). The lines serve as a guide to the eye.

As a last remark on the behaviour of the coercive field as a function of the dipolar strength at low temperatures, we have calculated the coercive field for the purely dipolar case, that is, $d = 0$ and $g = 1$. We have found the value $h_c = 1.98$, which is very close to the value 1.87 found by Russier [17] by the minimization of the dipolar energy at zero temperature.

4. Magnetic relaxation

In this section we present the results of the magnetic relaxation for an assembly of identical nanoparticles as a function of temperature and strength of the dipolar interaction. This subject has been investigated by Labarta's group through Monte Carlo simulations for different systems: non-interacting nanoparticles [29], non-interacting nanoparticles in an external magnetic field [28, 30], and chains of interacting nanoparticles [20, 31]. In these studies they considered the decay of the magnetization for a distribution of single-domain particles. The magnetization as a function of time is given by

$$M(t) = \int_0^\infty \exp(-t/\tau(E)) f(E)\, \mathrm{d}E, \tag{10}$$

where $f(E)$ is the distribution function of energy barriers and $\tau(E)$ is the relaxation time. The relaxation time [2], which is the average time to reverse particles' magnetization through the energy barrier, is given by

$$\tau(E) = \tau_0 \exp(E/k_B T), \tag{11}$$

where τ_0 is the time spent in a single attempt to overcome the energy barrier, and is of the order of nanoseconds. It is possible to show that

$$M(t) = \int_{E_c(t)}^{\infty} f(E)\,\mathrm{d}E, \tag{12}$$

that is, the magnetization decays in time according to the scaling variable $E_c(t) = k_B T \ln(t/\tau_0)$. Measurement of the magnetization as a function of temperature at a fixed time is equivalent to measuring the magnetization as a function of $\ln(t)$ for a fixed temperature. The validity of this scaling relation is restricted to cases in which the thermal energy $k_B T$ is very small compared with the width of the distribution $f(E)$. When this condition is satisfied it has been observed that the effect of magnetic fields and dipolar interactions is to decrease the effective energy-barrier height seen by the nanoparticles.

In the present study we are considering only identical nanoparticles, all with the same energy, E_0, for which the distribution of energy barriers is given by $f(E) = \delta(E - E_0)$. In this way the scaling law cannot be fulfilled at any physical temperature. The decay of magnetization is very simple and we can write

$$M(t) = M_0 \exp(-(t - t_0)/\tau), \tag{13}$$

where M_0 is the magnetization at an initial time t_0 and τ, for a fixed value E_0, becomes a function only of temperature. We will show below that, even without satisfying the scaling law, the dipolar interactions effectively reduce the height of the energy barrier seen by the nanoparticles. We must be careful in assuming a δ function for the energy barriers because the overall effect of dipolar interactions is to broaden the energy barrier distribution [20, 40]. Then, we restrict our analysis to the case of identical nanoparticles and small values of the dipolar strength. In this way, E_0 means the effective energy barrier of the distribution.

The initial configuration of the magnetic moments is the same as the one considered in the previous section in the study of remanence, that is, all the magnetic moments pointing in the x-direction, ($S_{ix} = 1$, $S_{iy} = 0$, $S_{iz} = 0$). This is possible after the application of a saturating magnetic field. At $t = 0$, the field is turned off and the system relaxes. Two very different relaxation regimes appear. The first one, almost independent of temperature, is very fast, and during it the magnetic moments try to find their most stable configuration. In the case of non-interacting particles the magnetic moments align along their easy axis, which is the lowest energy state for the system. After this initial regime, we enter the usual thermal relaxation, with the particles attempting to reverse their magnetic moments over the energy barriers. This process is very slow, especially in the region of low temperatures. We have considered the two regimes in the present study and we have monitored the decay of the magnetization during 10^4 MCSs. We have also taken averages over 200 samples, in order to take into account the different realizations of the uniaxial axis distribution.

We display in figure 14 the plots of the magnetization as a function of time for the non-interacting, $\alpha = 0$, and interacting, $\alpha = 0.1$, systems. After around 60 MCSs the system has already relaxed into its lowest energy state. As we have seen in the last section 10^4 MCSs corresponds to 200 ns and, in this way, we see that this very fast relaxation occurs within 1.2 ns, which is of the order of τ_0, and is not experimentally accessible. This plot also shows that the effect of dipolar interactions is to deviate the magnetic moments from the direction of their easy axis. For non-interacting particles the magnetization at the end of this fast relaxation is $1/2$, which is the expected value for a random distribution of uniaxial axes in three dimensions. To appreciate better the magnitude of the mean deviation of the moments from their easy axis direction, we plot in figure 15 the uniaxial anisotropy energy per particle as a function of the dipolar interaction strength. The mean deviation is given by $\langle \vec{e}_i \cdot \vec{S}_i \rangle$ and it increases smoothly with α. For instance, if $\alpha = 0.1$, the mean deviation is $\approx 6.5^\circ$.

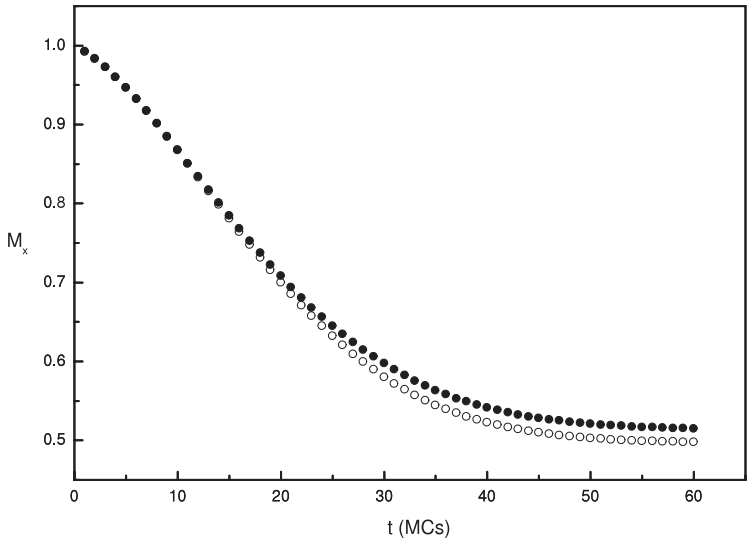

Figure 14. Ultrafast relaxation of the x-component of the magnetization for the interacting ($\alpha = 0.1$, solid circles) and non-interacting ($\alpha = 0$, open circles) systems.

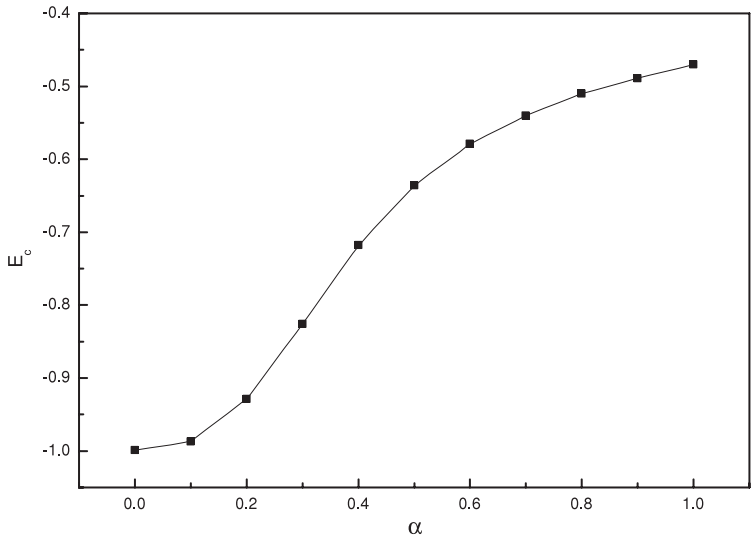

Figure 15. Uniaxial anisotropy energy per particle versus the dipolar interaction strength. The line serves as a guide to the eye.

In figure 16 we plot the logarithm of the x-component of the total magnetization as a function of time for the interacting system, $\alpha = 0.1$, and for different values of temperature. These curves are recorded after the initial time $t_0 = 60$ MCSs, for which the magnetization has the value M_0. At very low temperatures, $T = 0.02$ and 0.04 in our plot, the time of measurement is too small to observe appreciable changes in the magnetization and the data appear very noisy. At high temperatures the changes are visible but strongly nonlinear. For the intermediate range of temperatures, below the blocking temperature ($0.06 \leqslant T \leqslant 0.14$) the plots are approximately linear, and from the best linear fit to the curves the relaxation time (R_1)

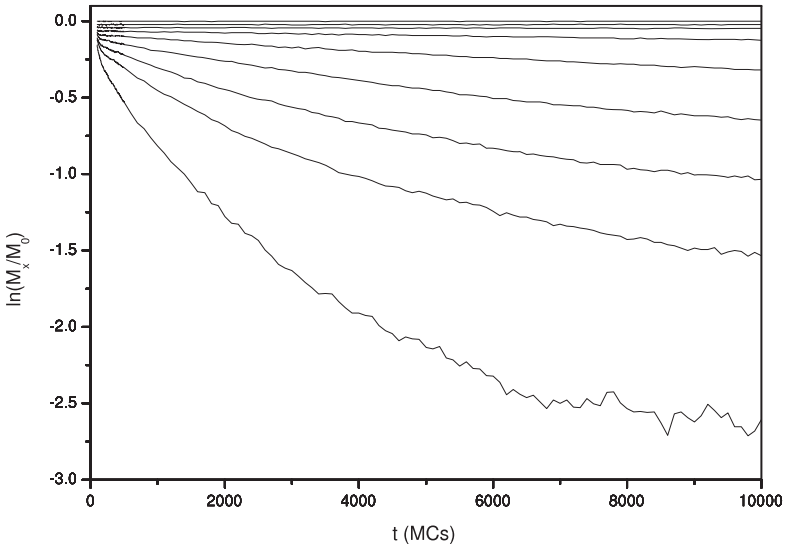

Figure 16. Slow relaxation of the x-component of the magnetization for the interacting ($\alpha = 0.1$) system for several values of temperature. $T = 0.02$ (topmost curve), $T = 0.2$ (bottom curve) in steps of 0.02 units.

is determined as a function of temperature. By plotting the magnetization curves for the non-interacting case, we have also determined the corresponding relaxation time (R_0) for the same intermediate values of temperature. Assuming the same microscopic time τ_0 for the interacting and non-interacting systems we can write

$$\ln\left(\frac{R_0}{R_1}\right) = \left(1 - \frac{d_1}{d_0}\right)\frac{d_0}{T}, \tag{14}$$

where $\frac{d_1}{d_0}$ is the ratio between the effective barrier heights of the interacting and non-interacting systems. Figure 17 shows the plot of $\ln(\frac{R_0}{R_1})$ versus the inverse of temperature, and from the best fit to the data we found $\frac{d_1}{d_0} = 0.67$. That is, for this particular relaxation process, we see that the energy barrier height for the interacting system is lower than that of the non-interacting one. This was already expected from an inspection of figure 15, which shows an effective mean deviation angle of the magnetic moments away from the easy axis, making easier the reversal of the magnetic moment through the uniaxial anisotropy barrier.

We have seen in section 3 that the ratio between the blocking temperatures of the most aggregated and well dispersed samples of magnetoferritin is 1.30, and this was in accordance with our calculations for $\alpha = 0.1$. There, the increase of 30% in the blocking temperature of the interacting system relative to the non-interacting one was related to an increase of the effective energy barrier due to the dipolar coupling [38]. Here, for the relaxation process, incidentally, we observe that the decrease in the energy barrier height of the interacting system relative to the non-interacting one is nearly the same, that is, 33%. Although our system is different from the one-dimensional model considered by Iglesias and Labarta [20], we have observed the same trend for the reduction of the effective energy barrier in the presence of dipolar interactions in the relaxation process. The effective energy barriers corresponding to the blocking temperature and to magnetization relaxation are different because the processes are different.

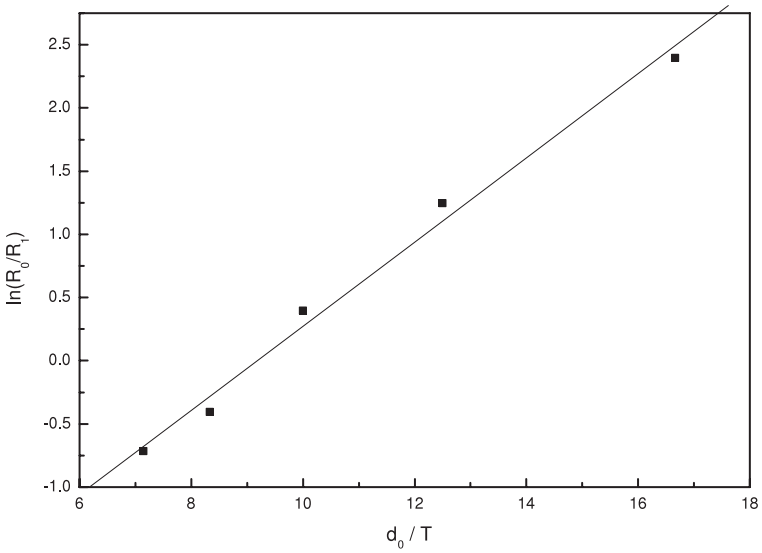

Figure 17. Dependence of $\ln(\frac{R_0}{R_1})$ on inverse of temperature along with the best fit to the data points. R_0 and R_1 are the relaxation times for the non-interacting and interacting systems, respectively.

5. Conclusions

We have studied the thermal properties and the relaxation of the magnetization of a system of identical nanoparticles arranged in a triangular lattice through Monte Carlo simulations. The uniaxial anisotropy axes of the particles are randomly oriented in three-dimensional space, and the magnetic moments are coupled by long-range dipolar forces. We have calculated the magnetization, susceptibility, specific heat and Binder cumulant as a function of temperature during a zero-field-cooling experiment. In the case of non-interacting particles we have seen that these thermal properties present a maximum at the blocking temperature of the array. We have also shown that the ratio between the blocking temperatures of the interacting and non-interacting systems is a decreasing function of the anisotropy energy for a given value of α. The remanence and the coercive field were also studied as a function of temperature and dipolar coupling strength. We have seen that we can determine the blocking temperature of the system by looking for the temperature at which the remanence and coercive field vanish. At very low temperatures the coercive field displays a minimum as a function of the dipolar field strength, which must be ascribed to the assumption of free boundary conditions in this work. We made this point clear by showing the development of a transverse component of the magnetization to field as a function of α. The ultrafast and slow relaxation regimes for the decay of the magnetization from a completely ordered state were also studied. We have shown that in the particular case of the relaxation process the effect of the dipolar interactions is to reduce the effective energy barriers seen by the nanoparticles to reverse their magnetic moments. We have applied our results to the magnetoferritin nanoparticles and we have found good agreement with recent measurements performed on this system.

Acknowledgments

WF acknowledges the enlightening discussions with Paul Southern on the magnetoferritin system. WF also acknowledges the scholarship from the Brazilian agency CNPq.

References

[1] Stoner E C and Wohlfarth E P 1948 *Phil. Trans. R. Soc.* A **240** 599
[2] Néel L 1949 *Ann. Geophys.* **5** 99
[3] Brown W F 1959 *J. Appl. Phys.* **30** 130S
[4] Hadjipanayis G C and Prinz G A (ed) 1991 *Science and Technology of Nanostructured Magnetic Materials* (New York: Plenum)
[5] Dormann J L, Fiorani D and Tronc E 1997 *Adv. Chem. Phys.* **98** 283
[6] Willard M A, Kurihara L K, Carpenter E E, Calvin S and Harris V G 2004 *Int. Mater. Rev.* **49** 125
[7] Petit C, Taleb A and Pileni M P 1999 *J. Phys. Chem.* **103** 1805
[8] Lin X M, Sorensen C M, Klabunde K J and Hadjipanayis G C 1998 *Langmuir* **14** 7140
[9] Meldrum F C, Heywood B R and Mann S 1992 *Science* **257** 522
[10] Wong K, Douglas T, Gider S, Awschalom D D and Mann S 1998 *Chem. Mater.* **10** 279
[11] Vargas J M, Nunes W C, Socolovsky L M, Knobel M and Zanchet D 2005 *Phys. Rev.* B **72** 184428
[12] Luo W, Nagel S R, Rosenbaum T F and Rosensweig R E 1991 *Phys. Rev. Lett.* **67** 2721
[13] Morup S and Tronc E 1994 *Phys. Rev. Lett.* **72** 3278
[14] Luttinger J M and Tisza L 1946 *Phys. Rev.* **70** 954
[15] MacIsaac A B, Whitehead J P, De'Bell K and Poole P H 1996 *Phys. Rev. Lett.* **77** 739
[16] De'Bell K, MacIsaac A B, Booth I N and Whitehead J P 1997 *Phys. Rev.* B **55** 15108
[17] Russier V 2001 *J. Appl. Phys.* **89** 1287
[18] Politi P, Pini M G and Stamps R L 2006 *Phys. Rev.* B **73** 020405
[19] Zhang X X, Wen G H, Xiao G and Sun S 2003 *J. Magn. Magn. Mater.* **261** 21
[20] Iglesias O and Labarta A 2004 *Phys. Rev.* B **70** 144401
[21] Robinson A P 2005 *PhD Thesis* University of Bristol
[22] Dimitrov D A and Wysin G M 1994 *Phys. Rev.* B **50** 3077
[23] Dimitrov D A and Wysin G M 1995 *Phys. Rev.* B **51** 11947
[24] Russier V, Petit C and Pileni M P 2003 *J. Appl. Phys.* **93** 10001
[25] Kechrakos D and Trohidou K N 1998 *Phys. Rev.* B **58** 12169
[26] Kechrakos D and Trohidou K N 2005 *Phys. Rev.* B **71** 054416
[27] Kechrakos D and Trohidou K N 2006 *Phys. Rev.* B **74** 144403
[28] Iglesias O and Labarta A 2002 *J. Appl. Phys.* **91** 4409
[29] Labarta A, Iglesias O, Balcells L and Badia F 1993 *Phys. Rev.* B **48** 10240
[30] Balcells L, Iglesias O and Labarta A 1997 *Phys. Rev.* B **55** 8940
[31] Ribas R and Labarta A 1996 *J. Appl. Phys.* **80** 5192
[32] Leite V S and Figueiredo W 2006 *Phys. Lett.* A **359** 300
[33] Leite V S, Grandi B C S and Figueiredo W 2006 *Phys. Rev.* B **74** 094408
[34] Ciftja O, Luban M, Auslender M and Luscombe J H 1999 *Phys. Rev.* B **60** 10122
[35] Ciftja O 2001 *J. Phys. A: Math. Gen.* **34** 1611
[36] Landau D P and Binder K 2000 *A Guide to Monte Carlo Simulations in Statistical Physics* (Cambridge: Cambridge University Press)
[37] Binder K 1981 *Z. Phys.* B **43** 119
[38] Kechrakos D and Trohidou K N 2002 *Appl. Phys. Lett.* **81** 4574
[39] Dimitrov D A and Wysin G M 1996 *Phys. Rev.* B **54** 9237
[40] Chubykalo-Fesenco O and Chantrell R W 2005 *J. Appl. Phys.* **97** 10J315